Neurochemical Research (2019) 44:2123–2138
https://doi.org/10.1007/s11064-019-02850-0

ORIGINAL PAPER

Experimental Characterization of the Chronic Constriction Injury-Induced Neuropathic Pain Model in Mice

Banulata Gopalsamy[1] · Yogesvari Sambasevam[1] · Nurul Atiqah Zulazmi[1] · Jasmine Siew Min Chia[1] · Ahmad Akira Omar Farouk[1] · Mohd Roslan Sulaiman[1] · Tengku Azam Shah Tengku Mohamad[1] · Enoch Kumar Perimal[1,2]

Received: 18 October 2018 / Revised: 3 July 2019 / Accepted: 29 July 2019 / Published online: 2 August 2019

Abstract

Number of ligations made in the chronic constriction injury (CCI) neuropathic pain model has raised serious concerns. We compared behavioural responses, nerve morphology and expression of pain marker, c-*fos* among CCI models developed with one, two, three and four ligations. The numbers of ligation(s) on sciatic nerve shows no significant difference in displaying mechanical and cold allodynia, and mechanical and thermal hyperalgesia throughout 84 days. All groups underwent similar levels of nerve degeneration post-surgery. Similar c-*fos* level in brain cingulate cortex, parafascicular nuclei and amygdala were observed in all CCI models compared to sham-operated group. Therefore, number of ligations does not impact intensity of pain symptoms, pathogenesis and neuronal activation. A single ligation is sufficient to develop neuropathic pain, in contrast to the established model of four ligations. This study dissects and characterises the CCI model, ascertaining a more uniform animal model to surrogate actual neuropathic pain condition.

Keywords Chronic constriction injury · Neuropathic pain · Allodynia · Hyperalgesia · Nerve degeneration · c-*fos*

Introduction

The use of animals as experimental models remains an integral part to resemble neuropathic pain in humans. Different models that have been well established over the years can represent neuropathic pain, a condition that arises due to injury at different regions of the nervous system. The sciatic nerve chronic constriction injury (CCI) remains one of the most commonly used models to study peripheral neuropathy [1–3]. This is because CCI is a well-established [4], reliable, easily reproducible [3] model that consistently exhibits symptoms of neuropathic pain. Furthermore, the CCI model has additional inflammatory components which is able to reproduce mixed aetiology of neuropathic syndromes [5], resulting in CCI being the model closest to mimicking the actual condition in human cases of neuropathy [6].

CCI is carried out by making loose ligations to the common sciatic nerve proximal to the trifurcation of the nerve at the mid-thigh level of the animal's hind limb [7]. These ligations are tightened just enough to 'reduce the diameter of the nerve and retard, but without causing interruption to the epineural circulation'. The CCI model first described by Bennett and Xie [7] was carried out by making four loose ligations in the sciatic nerve of rats. However, many studies have since been carried out in mice with modifications to the number of ligations. Some studies maintained the use of four ligations [8], while most studies in mice were carried out using three ligations [4, 9–13], two ligations [14] and only one ligation [15–17]. But, how these variations to the number of ligations affect the outcome of the CCI model remains questionable in comparison to the original model proposed by Bennett and Xie [7]. Is the ability of a drug to reduce pain responses tested in mice with single ligation as good as a model with four ligations? Even though the models developed with varying number of ligation to the nerve are able to demonstrate the required symptoms, the characteristics of pain surrogated by these models are undefined.

✉ Enoch Kumar Perimal
enoch@upm.edu.my

[1] Department of Biomedical Science, Faculty of Medicine and Health Sciences, Universiti Putra Malaysia, 43400 Serdang, Selangor, Malaysia

[2] Australian Research Council Centre of Excellence for Nanoscale BioPhotonics, University of Adelaide, Adelaide, SA 5005, Australia

The pathophysiology of neuropathic pain shows that an inflammatory reaction is triggered following nerve injury [18]. Inflammation is the body's natural reaction towards injury to remove the damaged tissue components and it is essential to initiate the repair process [19]. The inflammatory reaction causes the injured nerve to undergo degeneration, which in turn disrupts the normal pain transmission process. As a result, disproportionate and exaggerated pain impulses are transmitted—giving rise to neuropathic pain symptoms such as allodynia and hyperalgesia. Neurons along the pain transmission circuit are activated especially in regions that are highly related with pain perception [18]. This could be analysed by observing the c-*fos* expressions in the brain.

c-*fos* expression has been widely studied in researches related to pain for over 20 years. It is a useful marker for nociception [20] as it shows a specific, rapid and robust expression after noxious stimuli. c-*fos* is an immediate- early gene protein expressed within minutes by stimulation of a neurotransmitter [21]. Basal levels of c-*fos* in most cell types are relatively low but a dramatic increase in its expression occurs as a result of tissue injury or inflammation. A cascade of events is initiated following tissue injury where neurotransmitters or neuromodulators such as glutamate, brain-derived growth factor and substance P activates postsynaptic neurones. Then, central sensitization occurs following inhibition of potassium channel activities, increased NMDA and AMPA receptors, which in turn causes phosphorylation of extracellular signal-regulated kinase of dorsal horn neurones. Finally, transcriptional regulations of target genes such as c-*fos* is initiated [22].

In this study, we aim to characterize the CCI model and explore the behavioural responses to allodynia and hyperalgesia in murine species developed with one, two, three and four ligations respectively and investigate the necessity of numerous ligations on the sciatic nerve. Morphological alterations that occur within the nerve structure as well as the expression of c-*fos* in brain regions will provide a clearer picture to further review the model. We hope this study will provide further evidence on the use of this model to mimic peripheral neuropathy, and for the first time characterize the physiological and anatomical changes taking place within.

Materials and Methods

Animals

Male, seven to eight weeks old ICR mice with body weights ranging from 25 to 35 g were used in this study (Saintik Enterprise, Malaysia). Mice were acclimatized for a minimum of six days prior to any procedures and were subjected to conditions of 12 h light/ dark cycles (lights on at 8:00 a.m.). The room temperature remains at 24 ± 2 °C with humidity level of 70%. The animals were housed eight mice per cage and had free access to commercial feed and tap water. All procedures were carried out during the light phase (between 0900 and 1700 h). The experiments conformed to ethical guidelines for experiments involving pain in conscious animals and were carried out with the approval of Institutional Animal Care and Use Committee (IACUC) of Universiti Putra Malaysia (Reference number: UPM/IACUC/AUP-R060/2013).

Induction of Neuropathic Pain

Eighty animals were randomly divided into five groups with 16 mice in each group, as follows (i) sham group; CCI group with (ii) one ligation (iii) two ligations (iv) three ligations (v) four ligations. The surgery was performed under anaesthesia of tribromoethanol (250 mg/kg; intraperitoneal) with additional doses of anaesthetic given when required. Neuropathic pain was produced by the chronic constriction of the sciatic nerve as previously described by Bennett and Xie [7]. A small incision of approximately 1 cm was made on the skin at the middle thigh level before the biceps femoris and gluteus superficialis were separated by blunt dissection to expose the left common sciatic nerve. The injury was produced by tying loose ligatures according to their respective groups with 4/0 silk suture around the sciatic nerve, with 1 mm spacing between ligatures. The ligatures were tightened until the mice elicited a brief twitch in the hind limb. Iodine ointment was applied after the incision was closed with a non-absorbable suture. Mice allocated in sham group had the entire surgery performed without the ligatures. The mice were then returned to their home-cages after recovery and were inspected daily.

Nociceptive Assays

Mice (n = 8 mice from each group) were trained for all the behavioural tests for two consecutive days. Baseline measurements (pre-CCI threshold/ latency) were obtained one day before CCI. Post-CCI threshold/latency was obtained weekly for a period of twelve weeks.

Mechanical Allodynia

Response towards mechanical allodynia was assessed based on the responsiveness of the hind paw to the application of automated electronic von Frey filaments (IITC Life Science Inc., CA, USA) as described by Vadakkan et al. [23]. Mice were placed on a wire mesh grid and were allowed to acclimate for 30 min prior to testing. von Frey filament was applied to the middle of the dorsum of the foot while the animal is on its four limbs. The withdrawal threshold was obtained from ipsilateral paw. The mean of three readings

was obtained for each paw with an interval of 5 min between each reading.

Cold Allodynia

Cold allodynia was measured using the cold plate test. Each mouse was placed on the cold plate (Ugo Basile, Italy) which was pre-set at a temperature of 5 °C [7, 24]. The number of times the mouse lifts up or flinches its paw was recorded for duration of 5 min. The scores were obtained by subtracting the contralateral paw lifts count from the ipsilateral paw lifts count.

Mechanical Hyperalgesia

Mechanical hyperalgesia was evaluated using Randall–Selitto test as described by Randall and Selitto [25]. Each mouse was restrained as such that it was able to flex its legs and pressure was applied on the plantar surface of the mouse's foot through the tip of the analgesy meter (IITC Life Science Inc., CA, USA). Pressure by the tip was increased at a constant rate until the animal struggles, squeals or attempts to bite and values were recorded as the pain threshold. To ensure further injury to the paws are avoided, a cut off force was set at 200 g.

Thermal Hyperalgesia

Thermal hyperalgesia was assessed using Hargreaves' test as described by Hargreaves et al. [26] using Hargreaves apparatus (37,370, UgoBasile, CA, USA). Mice were acclimatized for 30 min on an elevated platform with a clear glass top. A radiant heat source with an infrared intensity of 80 W/sr was directed to the middle plantar of the animal's ipsilateral limbs, one at a time. The duration for the mice to withdraw its paw from the heat source was measured as its paw withdrawal latency of thermal hyperalgesia. A cut-off time of 20 s was set, after which the heat source was removed to prevent heat damage to the skin.

Nerve Morphometric Analysis

Animals (n = 5) of all groups were sacrificed on Day 15 following induction of neuropathic pain (CCI). Approximately 1 mm^3 of the sciatic nerve proximal to the spinal cord was dissected out within 2 min after the mice was decapitated and was fixed in 4% gluteraldehyde for 24 h at 4 °C. The specimens were then post fixed with osmium tetroxide (OsO_4), dehydrated in a graded series of acetone before embedding in resin mixture. Polymerisation was initiated by heating in an oven at 60 °C for 48 h. Semithin (1 µm) sections were obtained using an ultramicrotome (Leica UC6, Holland) and were stained with 1% toluidine blue. The sections were then observed under light microscope (Leica, Germany) at × 40 magnification and five regions of 50 µm × 50 µm were determined to carry out measurements. Since many structural changes were observed at the outer region of the nerve cross section, samplings were made at five regions along a straight line that passes through the centre of the nerve cross section to equalize the selection from all regions of the nerve. The images were measured using ImageJ software (NIH Image 1.47; U.S. National Institutes of Health, Bethesda, MD, USA). Diameter of both axons and fibres were normalized using the equation diameter = perimeter/π to obtain unbiased measurement based on the circularity as this equation considers the irregular shaped axons and fibres as previously stated by Liang et al. [27]. Perimeter and area of each axon and fibre were obtained by digitally tracing around the perimeter of the axonal membrane and myelin sheath respectively. G-ratios were obtained by dividing the axonal perimeter by its corresponding fibre perimeter. Degenerative profiles in the samples were identified as axons with folded myelin/tomacula, onion bulb formations of myelin sheath, detachment of the myelin sheath from the basal lamina and extensive myelin degeneration.

c-fos Immunoreactivity

Day 15 post-CCI, six mice from respective groups, which were not subjected to nociceptive assays were deeply anaesthetized using tribromoethanol (> 250 mg/kg, intraperitoneally) and perfused transcardially with 0.1 M phosphate buffered saline (PBS) followed by 10% neutral buffered formalin (NBF, pH 7.4) for 10 min. The frontal brain was dissected out and post fixed in the same fixative for 24 h. Organs were processed and embedded in paraffin wax. Coronal sections of the brain at a thickness of 5 µm were mounted onto positive charged APES polycoated slides. Staining for c-*fos* immunopositive cells were then carried out. Sections were dewaxed, hydrated and incubated in 1% H_2O_2 Peroxidase (DAKO, USA) for 20 min and rinsed thoroughly in 0.1 M Tris-buffered saline (TBS; pH 7.4). After incubation in 3% BSA (Sigma, USA) for 1 h, the sections were incubated with c-*fos* polyclonal antibody (Abcam, 1:100) for 1 h at room temperature. After several rinses in TBS, sections were incubated with secondary substrate with polymer for 30 min (DAKO, USA). This was followed by a thorough washing of the sections before incubation with chromogen 3,3′-diaminobenzidine tetrahydrochloride (DAB, DAKO, USA) for 10 min. Slides were then counterstained with Mayer Hematoxylin, dehydrated, cover slipped and analysed under light microscope (Leica, Germany) at × 10 magnification. c-*fos* quantification was carried out on bilateral sides at four regions of the frontal brain which include cingulate cortex, parafascicular nuclei, amygdala and the hippocampus as shown in Fig. 1. Identification of the brain regions

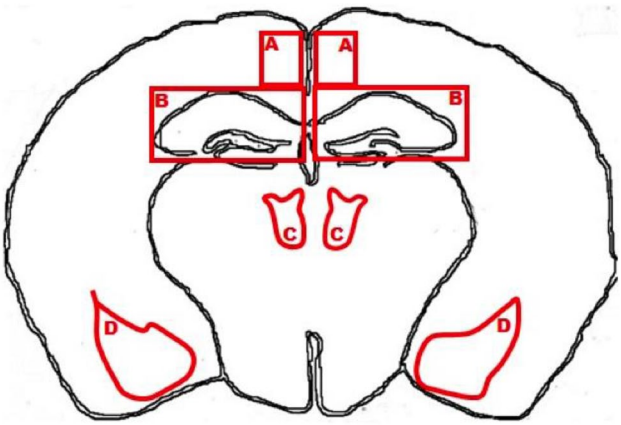

Fig. 1 Schematic depiction of the brain coronal section at Interaural: + 1.68 mm and Bregma: − 2.12 mm illustrating **a** Cingulate cortex, **b** Hippocampus, **c** Parafascicular nuclei and **d** amygdala

were carried out with reference to the Paxinos and Franklin [28] mice brain atlas, in coronal sections approximately (Interaural: + 1.68 mm and Bregma: − 2.12 mm). Ten non-overlapping areas in each region were randomly selected using microscopic 100 µm × 100 µm square grids and the c-*fos* immunoreactive positive stained nuclei within the area were counted manually. Staining was carried out across the groups where every batch contained at least one brain section of mice from each group.

Statistical Analysis

All analysis was performed using SPSS software (Chicago, IL) and data are expressed as mean ± SEM. Statistical significance was determined by two-way ANOVA followed by Bonferroni's post hoc analysis. Nerve morphometric analysis was analysed using Mann–Whitney test. A confidence interval of 5% or less was considered to be statistically significant. All behavioural tests, nerve morphometric analysis and c-*fos* counting were carried out where the investigator was blinded from the treatment group of the animals.

Results

Nociceptive Assays

To investigate the influence of varying number of constrictions to the sciatic nerve on the development of neuropathic pain symptoms, we assessed the behavioural responses of mice with CCI-induced with different number of ligation(s) throughout a period of 12 weeks. Accordingly, as shown in Fig. 2a, mechanical allodynia developed in three and four ligations CCI-induced mice as early as day 7 and was present in all groups on day 14. Response towards mechanical allodynia was at its peak levels on day 14. Interestingly, in all cases, the withdrawal threshold values were similar ($p > 0.05$) indicating no differences between the numbers of ligation(s) employed to develop the model.

When the development of cold allodynia was assessed, we observed all CCI-induced with different number of ligation(s) mice to have significantly ($p < 0.05$) higher number of paw lifts compared to the sham group indicating more pain (Fig. 2b). The increased pain response was observed from day 7 and is also reported to be at peak levels on this day after which the values reduced gradually. On day 14, mean values of paw lifting in the one, two, three and four ligation groups were 8.17 ± 1.01, 6.67 ± 0.61, 9.00 ± 1.06 and 8.00 ± 0.58 respectively, whereas sham group recorded a mean value of 0.00 ± 0.00.

Response towards mechanical hyperalgesia was also tested in mice with different number of ligation(s). As shown in Fig. 2c, this symptom developed earlier in CCI mice with four ligations with mean withdrawal threshold of 133.5 ± 2.75 g on day 7 which was significantly lower ($p < 0.05$) than the other groups. Nevertheless, by day 14 all CCI-induced with different number of ligation(s) mice successfully developed mechanical hyperalgesia, which was present throughout the experimental period of 84 days.

All mice subjected to CCI developed thermal hyperalgesia as shown in Fig. 2d. Lowest withdrawal latencies in CCI groups were recorded on day 14, 21, 28 after which the withdrawal latency gradually increased over time until the end of the experimental period. Mice with four ligations showed thermal hyperalgesia as early as day 7 with mean withdrawal latency of 7.95 ± 0.19 s. This pain response was totally diminished in all groups by day 84. However, there were no significant differences ($p > 0.05$) in paw withdrawal latencies between groups with different number of ligation(s) indicating the number of ligation(s) made to the sciatic nerve did not affect the response towards thermal hyperalgesia.

Nerve Morphology

Table 1 shows the total number of fibres, fibre density, fibre diameters, axon diameters, myelin thickness and g-ratio of myelin thickness were not altered ($p > 0.05$) by the injury to the sciatic nerve. However, area of the fibre and axons were significantly ($p < 0.05$) lower compared to the sham group thus an increase in the endoneurial area within sampled field could be observed in Fig. 3. The profiles that indicate degeneration of the nerve fibres were present in significant ($p < 0.05$) numbers in ligated nerves compared to the sham group.

Figure 4a translates the distribution of fibre diameter in sciatic nerves 14 days post CCI. The sham group demonstrates a normal distribution as 62.7% fibres in sham group falls in the category of larger diameter (6–19 µm)

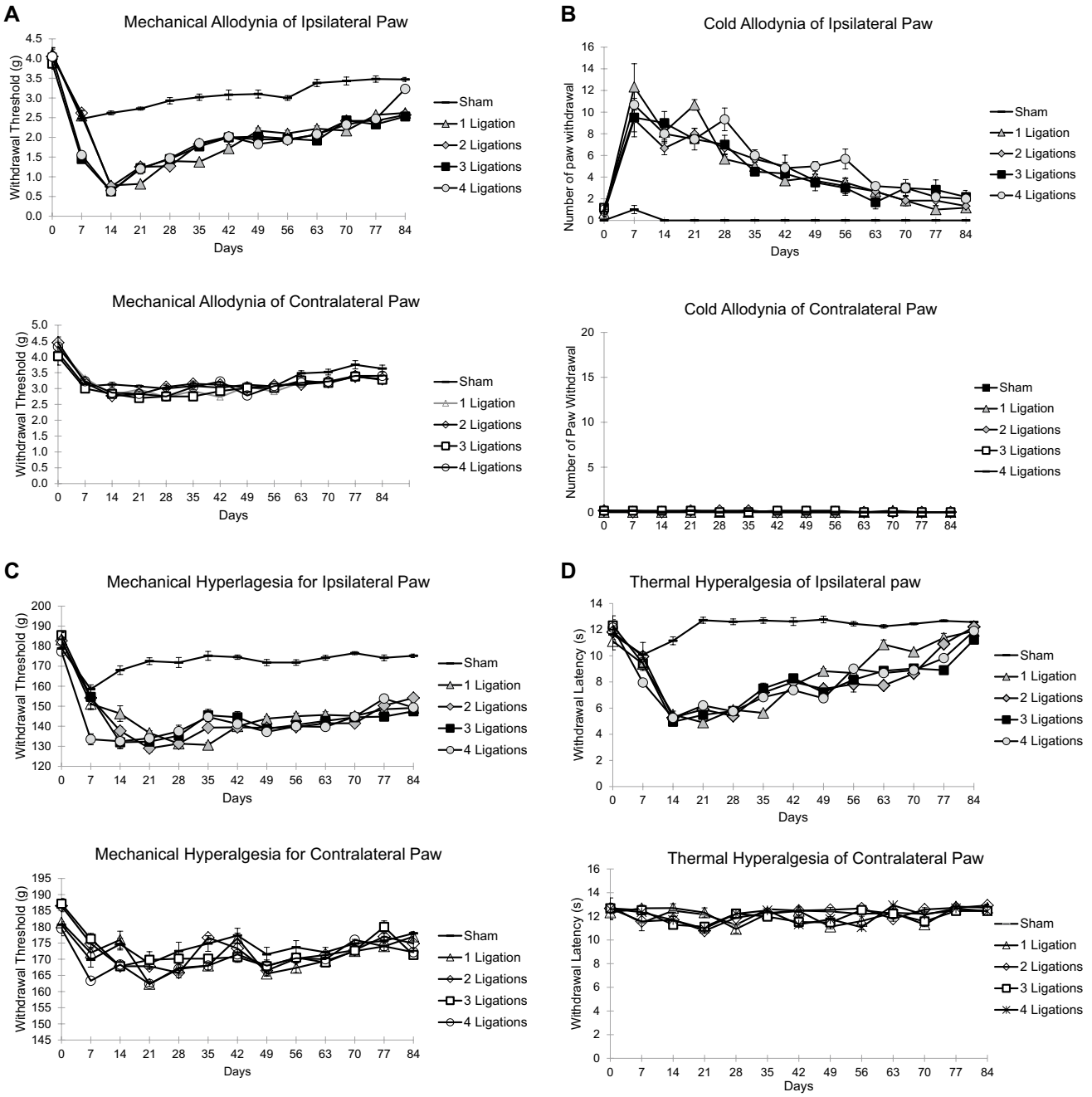

Fig. 2 Ipsilateral and contralateral paw withdrawal threshold in response to **a** mechanical allodynia, **b** cold allodynia, **c** mechanical hyperalgesia and **d** thermal hyperalgesia in chronic constriction injury-induced mice with one, two, three or four ligation(s). Results are shown as mean values ± SEM; n = 8 animals per group, assessed by two-way ANOVA followed by Bonferroni's post hoc analysis. Filled shapes indicate significant difference ($p < 0.05$) from sham group

compared to 53.8, 47.5, 51.9 and 37.8% in one, two, three and four ligation(s) groups, respectively. The distributions of fibre diameters in all the ligated groups are shifted to the left indicating 45.5, 50.9, 44.8 and 61.5% of fibres in one, two, three and four ligation(s) groups, respectively fall in the smaller diameter (0–6 µm) category compared to sham that recorded only 30.7% fall within this category.

Figure 4b illustrates the distribution of axon diameter of myelinated fibres. Sham group showed that 23.7% axons fall in the 3–4 µm range whereas in the ligated groups, highest count of axons had diameters of 2–3 µm 21.2, 21.1, 20.3 and 29.0% in one, two, three and four ligation(s) groups, respectively compared to only 13.5% axons in sham group falls in this range. There is a shift towards

Table 1 Morphometric of the sciatic nerve cross section on the ipsilateral side proximal to spinal cord in CCI mice with different number of ligations and sham control on day 14 post CCI

	Sham	1 ligation	2 ligations	3 ligations	4 ligations
Total fibre number (in 5 regions)	224.67 ± 8.11	135.00 ± 3.06	170.33 ± 32.46	182.33 ± 40.53	153.00 ± 27.30
Fibre density (no/mm^2)	17,973.00 ± 648.828	10,800.00 ± 244.404	13,626.67 ± 4498.059	14,586.67 ± 3242.057	12,240.00 ± 2184.063
Fibre diameter (μm)	6.90 ± 0.11	6.75 ± 0.23	6.84 ± 0.55	7.06 ± 0.53	6.16 ± 0.16
Axon diameter (μm)	4.30 ± 0.21	4.31 ± 0.24	4.35 ± 0.30	4.62 ± 0.43	3.81 ± 0.11
Fibre area (area/2500 μm^2)	1577.91 ± 8.39^a	880.19 ± 35.60^b	1036.09 ± 26.38^b	1061.06 ± 41.47^b	894.60 ± 84.30^b
Axon area (area/2500 μm^2)	592.52 ± 33.04^a	294.02 ± 15.51^b	365.34 ± 19.60^b	381.34 ± 36.68^b	255.29 ± 53.72^b
Endoneurial area (μm^2)	922.09 ± 8.39^a	1626.47 ± 29.12^b	1463.91 ± 26.38^b	1438.94 ± 41.47^b	1602.40 ± 85.83^b
Myelin thickness (μm)	2.60 ± 0.11	2.43 ± 0.05	2.48 ± 0.26	2.45 ± 0.11	2.35 ± 0.10
Myelin area (μm^2)	22.43 ± 0.14	19.71 ± 0.67	21.85 ± 3.84	20.71 ± 2.26	17.93 ± 1.25
g-ratio	0.6081 ± 0.03	0.61 ± 0.01	0.62 ± 0.02	0.63 ± 0.01	0.60 ± 0.01
Degenerative profile (no.)	2.80 ± 0.72^a	15.13 ± 2.22^b	19.80 ± 4.61^b	18.6 ± 1.10^b	14.53 ± 1.62^b

Results are shown as mean values ± SEM; n = 6 animals per group

^{a,b}Values within the same row with different superscripts are significantly different at ($p < 0.05$)

smaller diameter range in ligated groups compared to a normal distribution of sham group. Ligations made to the sciatic nerve also caused structural changes in myelin thickness on day 14 post-CCI as shown in Fig. 4c. A similar trend was also observed in the distribution of fibre and axonal diameters where the sham group shows a normal distribution but the graph skewed towards the smaller ranges in ligated groups. Curves of ligated groups were shifted to the left indicating thinner myelin sheath. Note also that sham group had smaller range of myelin thickness indicating the fibres were more uniform in shape and thickness of myelin. Ligated groups however recorded a wider range of myelin thickness indicating some myelin were undergoing degeneration while some myelin showed thickening. This result shows that the myelin sheaths underwent degeneration when the nerves were subjected to ligations.

c-fos Expression

Figure 5 shows the expression of c-*fos* positive stained nuclei in four regions of mice brains. The quantification of c-*fos* positive cells revealed increased ($p < 0.05$) expression in the cingulate cortex (Fig. 6), parafascicular nuclei (Fig. 7) and amygdala (Fig. 8) regions of the brain in CCI mice compared to sham mice. Quantification of the stained cells did not show significant difference ($p > 0.05$) among the different CCI models. As shown in Fig. 5, the number of c-*fos* positive nuclei hippocampus (Fig. 9) region of the brain is 24.8 ± 3.02, 29.6 ± 3.4, 32.2 ± 3.15, 28.2 ± 3.32 and 27.6 ± 3.33 in sham, one, two, three and four ligation groups respectively. The count showed no changes ($p > 0.05$) between the sham and ligated groups.

Discussion

The CCI model is widely used in neuropathic pain research. Even though the models were developed with varying number of ligations and all the models were able to surrogate symptoms of allodynia and hyperalgesia, it is essential for us to validate these CCI models under one experimental condition. This is to rule out possible confounding factors that might be present. Subjectivity in terms of materials and surgical techniques used, order of testing as well as techniques of the experimenter could be controlled. Besides that, factors from the animals such as diet, age, gender, strain and species specificity, and stress reactivity could be eliminated. The use of different suture materials to ligate the nerves demonstrates varying outcomes in different animal models. More stable neuropathic pain behaviours are mimicked when silk sutures were used in murine models [29] and catgut ligatures in rat models [30]. Therefore, we standardise the laboratory environment which has a robust effect on behaviour traits [31] enabling us to characterise the model in an unbiased manner.

The outcome shows that all the CCI models displayed symptoms of neuropathic pain in line with previous studies [8, 13–15]. The pathophysiology of neuropathic pain shows that pain is developed mainly as a result of the inflammatory microenvironment and release of mediators [32] at the site of injury that is initiated by the suture material [7] rather than the nerve injury itself. Neuropathic pain is caused by the failure of nerve-blood barrier in maintaining the

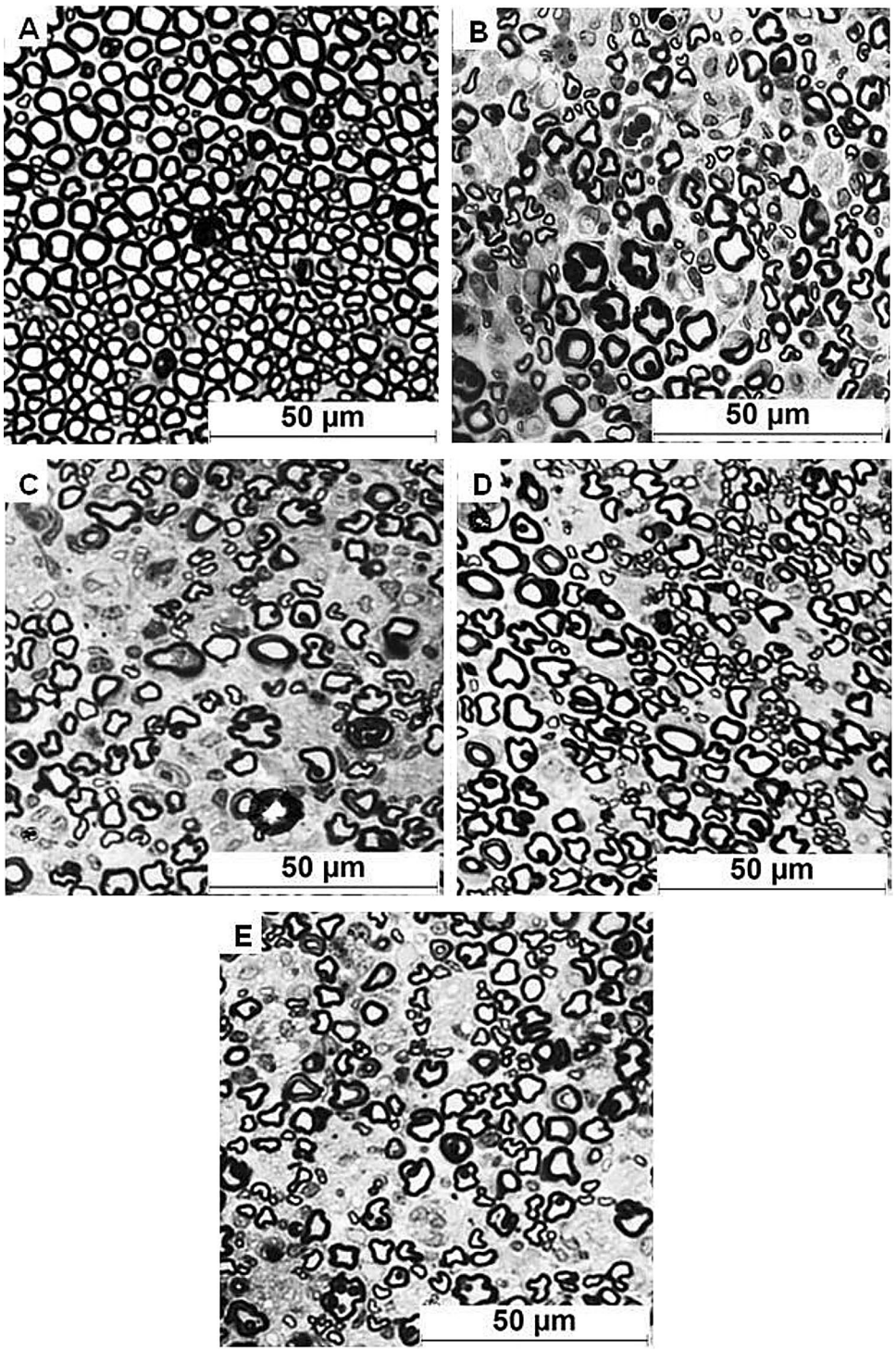

Fig. 3 Semi-thin sections of toluidine blue-stained mice sciatic nerves 14 days post CCI of **a** sham-operated, **b**–**e** CCI mice with one, two, three and four ligation(s) respectively, n = 6 animals per group. Myelin sheaths in the ligated nerves appear irregular, elongated and collapsed compared to the sham control, which shows a more regular and rounded shape. The endoneurium space is increased in ligated groups with the presence of numerous basal lamina compared to sham control which has a more compact arrangement of fibres

construction of the inner peripheral nerve whereby it also modulates the infiltration and concentration of ions causing local inflammation and leakage [33]. Inflammation initiates the release of mediators such as bradykinin, prostaglandins, substances P and cytokines. These mediators cause sensitization of the primary afferent neurons, lowering the threshold for propagation of action potential, and increasing the firing rate of action potential thus perceiving non-noxious stimuli as noxious, allodynia; and exhibiting disproportionate hypersensitivity to noxious stimuli, hyperalgesia; which are two characteristics of neuropathic pain [34].

A study by Maves et al. [35] demonstrated that thermal hyperalgesia, allodynia and guarding behaviour commonly observed in animals with neuropathic pain could be present

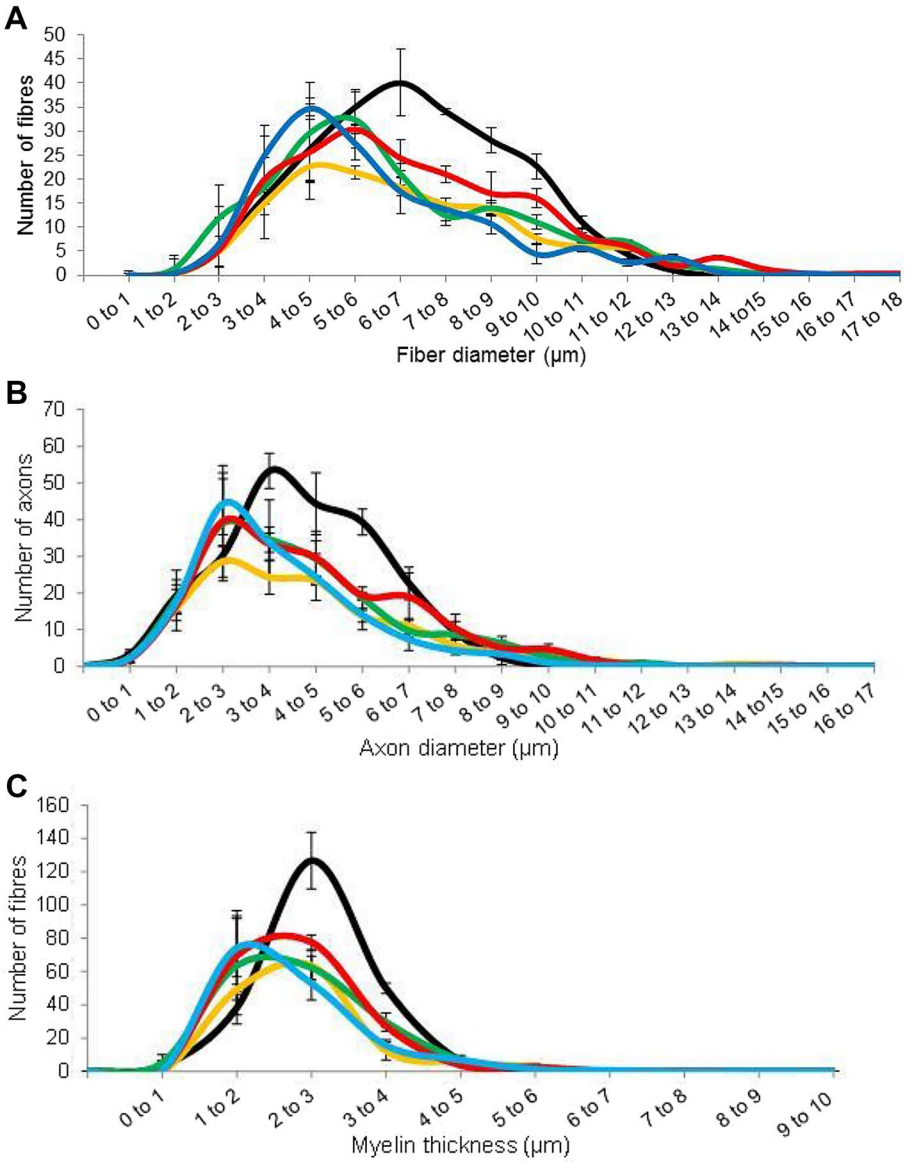

Fig. 4 Analysis on **a** fibre diameters, **b** axon diameters and **c** myelin thickness of myelinated fibres in sciatic nerve 14 days post CCI from sham (black line), one ligation (yellow line), two ligations (green line) three ligations (red line) and four ligations (blue line) groups. Note that curve of sham control group is shifted to the right indicating more fibres recorded larger diameters/thickness. Curves of ligated groups were shifted to the left indicating most fibres had smaller diameter/thickness. Data are presented as mean ± SEM, n = 6 animals per group (Color figure online)

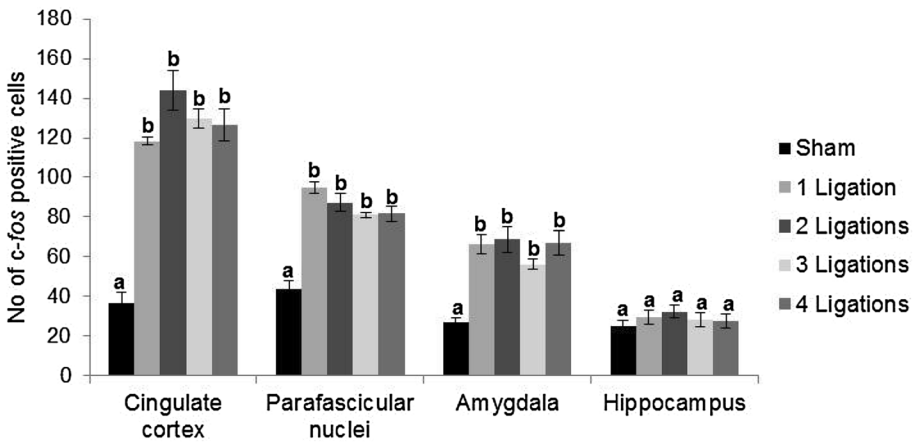

Fig. 5 Number of c-*fos* positive immunoreactivity in the cingulate cortex, parafasicular nuclei, amygdala and hippocampus regions in the brain Sects. (100 μm × 100 μm × 10 regions). Results are shown as mean ± SEM, n = 6 animals per group. [abc]Columns with different superscripts are significantly different at ($p < 0.05$)

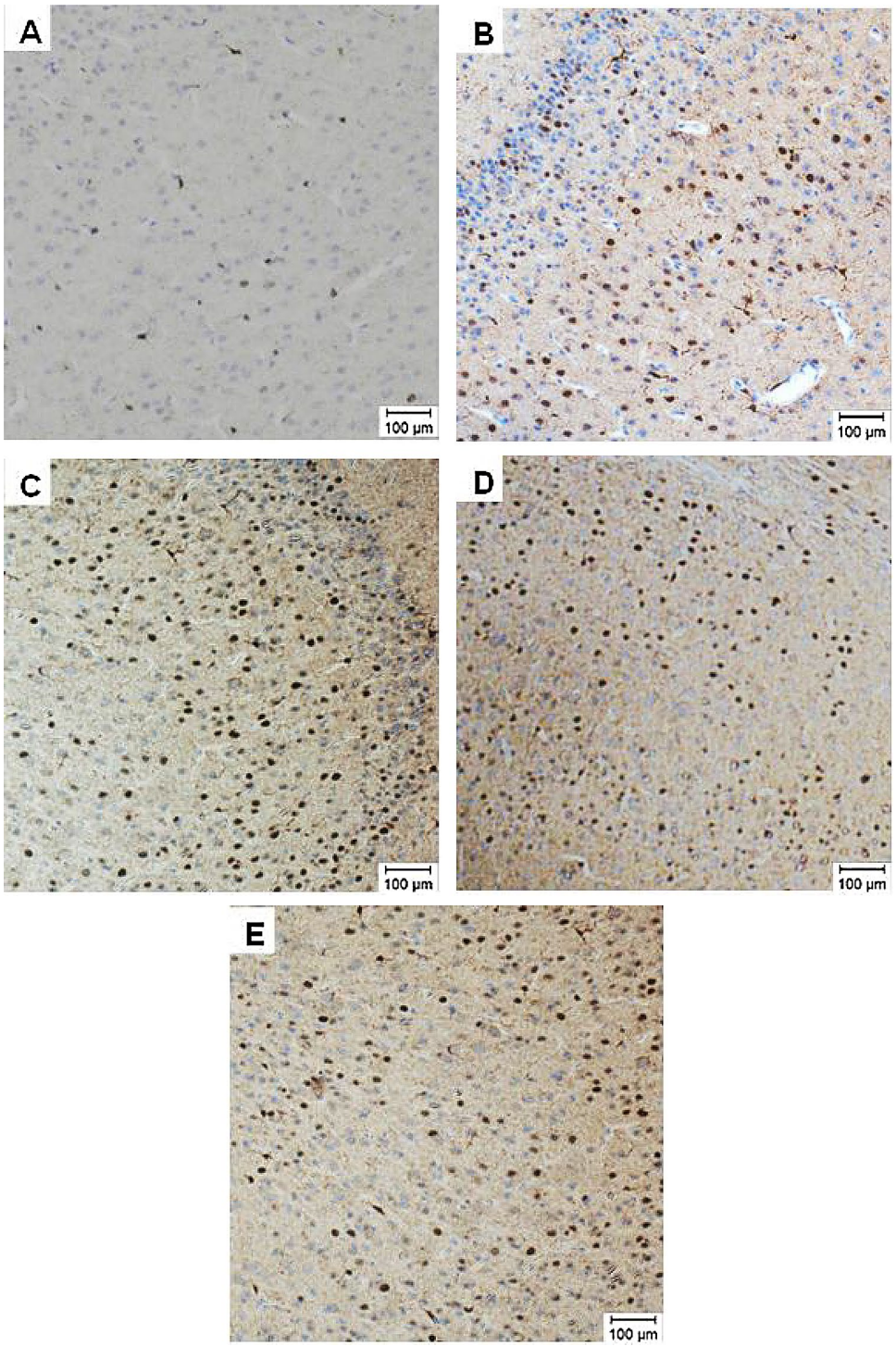

Fig. 6 Photomicrographs of c-*fos* immunopositive cells (cell nucleus with brown colouration) in the cingulate cortex region in coronal sections at around Interaural: + 1.68 mm and Bregma: − 2.12 mm. mice brain 14 days post CCI of **a** sham-operated, **b**–**e** CCI mice with one, two, three and four ligations respectively, n = 6 animals per group. Immunohistochemistry staining at × 10 magnification (Color figure online)

when chromic gut sutures were merely laid adjacent to the sciatic nerve [35, 36]. However, hyperalgesia and allodynia were generally absent with the use of silk or plain gut in that study. Kajander et al. [37] therefore suggested that interaction between chemical components, specifically chromic salts and pyrogallol from chromic gut sutures and the sciatic/sympathetic nerves leads to the inflammatory reaction that causes neuropathic pain. However much later from the study by Maves et al. [35], Yamashita et al. [38] confirmed that this pain condition could be induced by every suture material with very minimal difference between silk, chromic, ethilon, nurolon, monocryl or coated vicryl. Therefore, the hypothesis that pharmacological or chemical reaction triggers the development of neuropathic pain in CCI model has

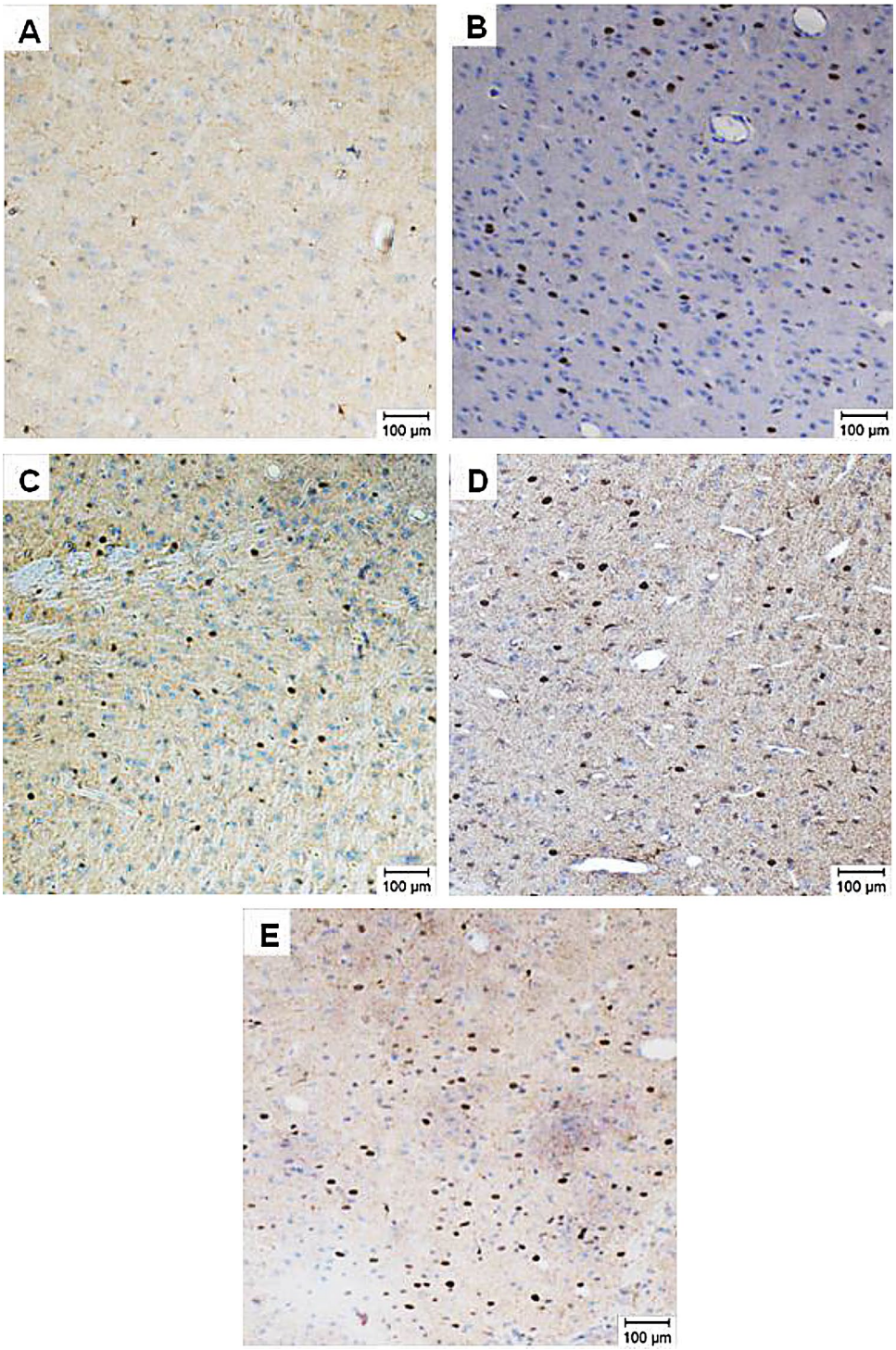

Fig. 7 Photomicrographs c-*fos* immunopositive cells (cell nucleus with brown colouration in the parafascicular nuclei region in coronal sections at around Interaural: + 1.68 mm and Bregma: − 2.12 mm of the mice brain 14 days post CCI of **a** sham-operated, **b**–**e** CCI mice with one, two, three and four ligations respectively, n = 6 animals per group. Immunohistochemistry staining at × 10 magnification (Color figure online)

to be reconsidered, as more evidences are apparent that the mechanical factors might be associated. Furthermore, the suture material used for surgeries and implants are generally absorbed and eventually loses the tensile strength. Silk however has been reported to have a lower rate of absorbance whereby a complete intact suture could still be observed histologically after 2 years of implantation [39].

Maves et al. [35] reported the presence of a "dose-dependent'' hyperalgesia and allodynia when different lengths of chromic gut sutures were aligned along the sciatic nerve in rats. However, here we report "all-or-none" pain symptoms as the magnitude of pain thresholds and latencies were similar, regardless of the number of ligation(s) made to the sciatic nerve. Display of allodynia and hyperalgesia were

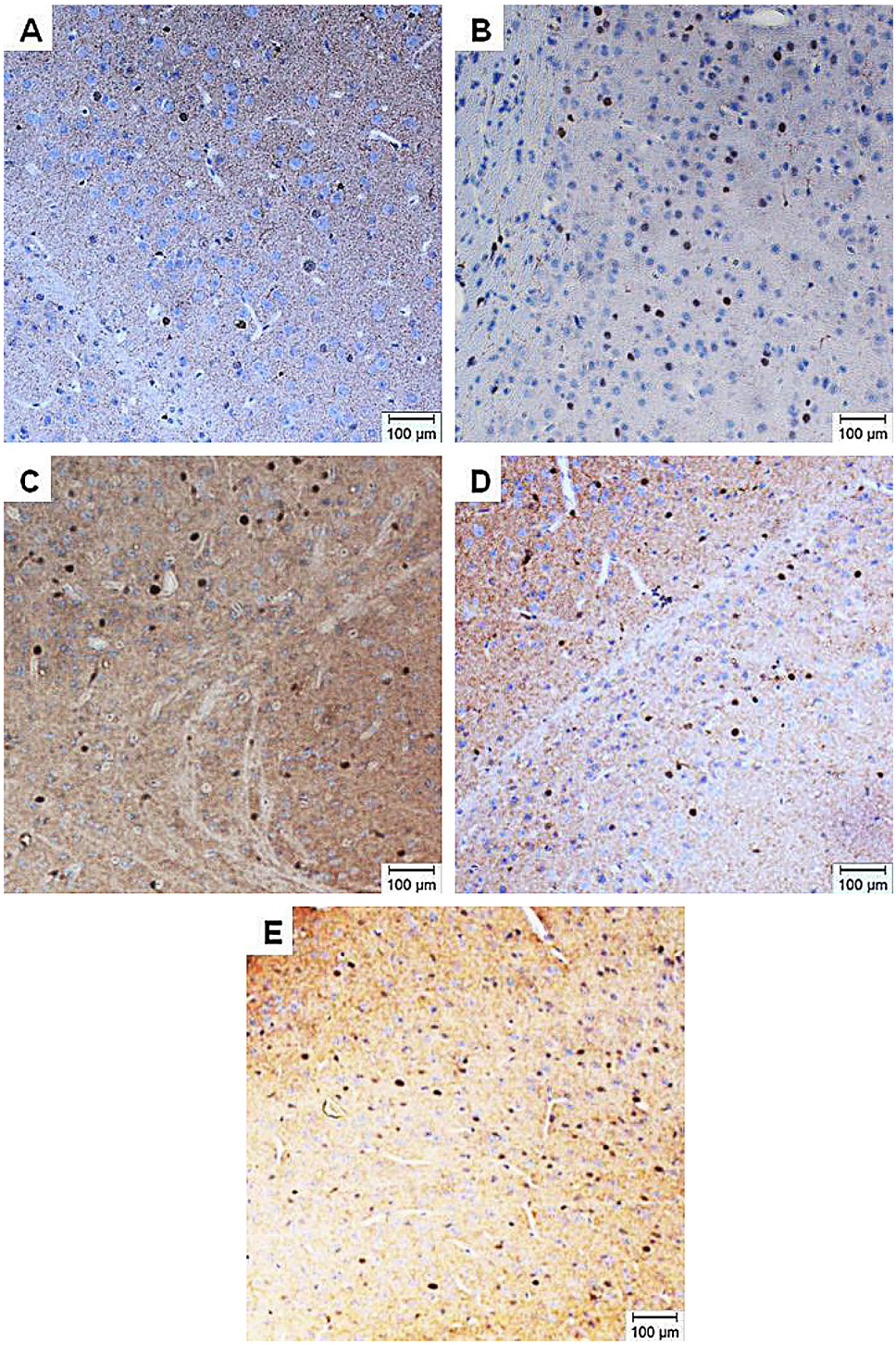

Fig. 8 Photomicrographs c-*fos* immunopositive cells (cell nucleus with brown colouration in the amygdala region in coronal sections at around Interaural: + 1.68 mm and Bregma: − 2.12 mm of the mice brain 14 days post CCI of **a** sham-operated, **b**–**e** CCI mice with one, two, three and four ligations respectively, n = 6 animals per group. Immunohistochemistry staining at × 10 magnification (Color figure online)

more stable on day 14 indicating that all the CCI models are competent to be used at this time point. Furthermore, peak responses were observed on day 14, similar to that reported by Jaggi and Singh [40]. This is an ideal time period for behavioural testing as inflammation due to the skin incision made during the surgery would have dissipated by this time, thus the pain response exhibited fully represents neuropathy [41].

The ultrastructural changes within the sciatic nerve further gave an insight on pathophysiological changes that takes place at the injury site. Following nerve compression, axons degenerate both at the distal (orthograde/Wallerian degeneration) and proximal (retrograde degeneration) region of the injury [42]. Degeneration of the nerve distal to the injury is more prominent whereby a total axonal loss could be observed as early as day three post injury [43].

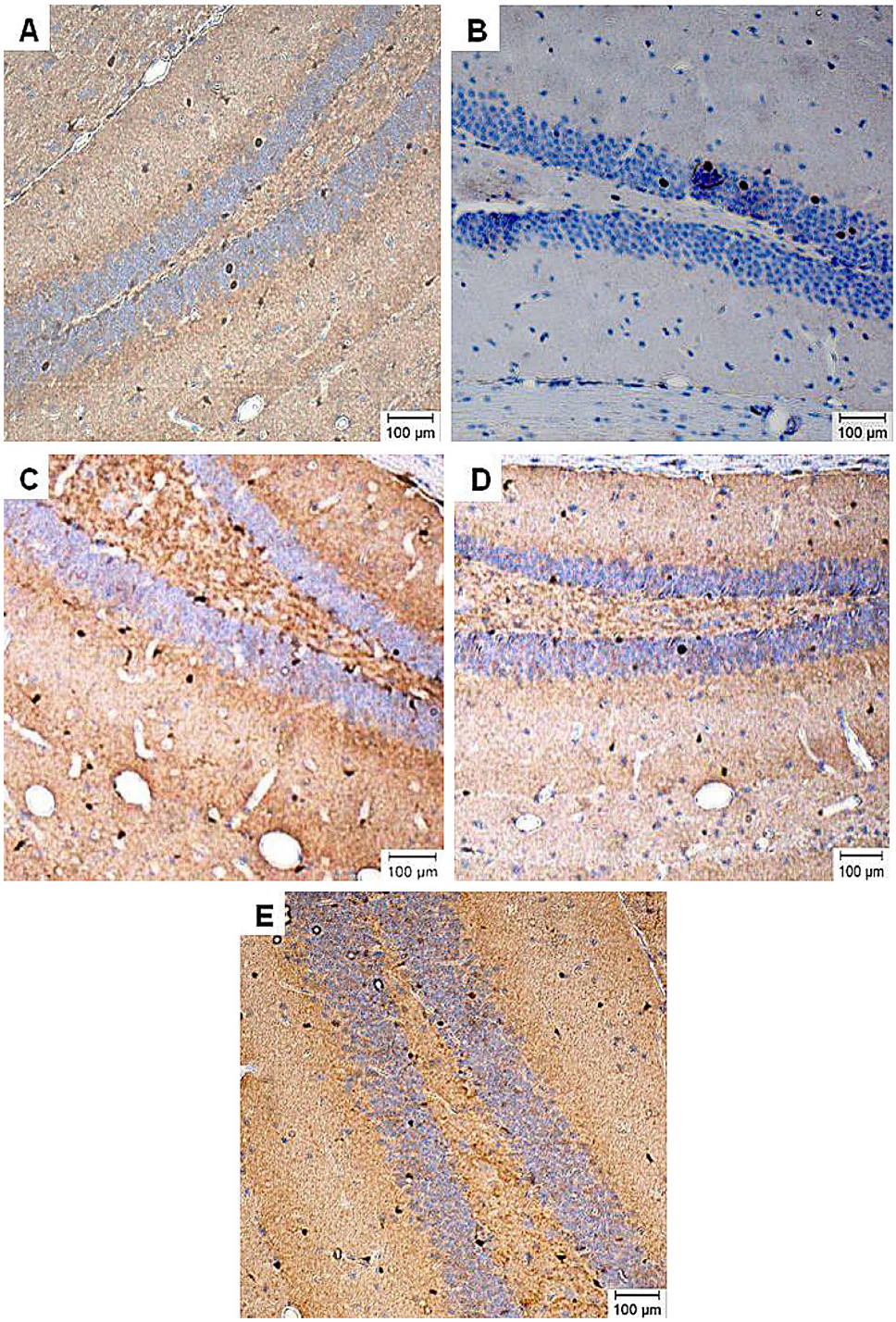

Fig. 9 Photomicrographs of c-*fos* immunopositive cells (cell nucleus with brown colouration) in the hippocampus region mice brain 14 days post CCI of **a** sham-operated, **b–e** CCI mice with one, two, three and four ligations respectively, n = 6 animals per group. Compact dentate granule cells indicate the dentate gyrus region in coronal sections at around Interaural: + 1.68 mm and Bregma: − 2.12 mm. c-*fos* immunopositive cells (brown colour nucleus) are present both in the dentate granule cells and area surrounding it. Immunohistochemistry staining at × 10 magnification (Color figure online)

The proximal region however, has more intact structures, which could be quantitatively analysed. The axonal number was indifferent in neuropathic mice and sham control, but a lower proportion of large-size fibres and bigger proportion of small-size fibres were observed when the nerves were ligated, probably due to sprouting which occurs after injury [44]. Moreover, axons in the ligated nerves appear irregular and shrunk as the rapid degeneration process begins with degeneration of axonplasm and axolemma. This causes the integrity of the axonal structure to be compromised following granular disintegration of the cytoskeleton [45], causing the structure to collapse into the axonplasm. Schwann cells that tightly wrap around the axons forming myelin sheath loses its tightness between the layers, as increased amounts of longitudinally oriented collagen fibres are present between layers of the Schwann cells. This occurs as an

effect of sequential segmental demyelination and remyelination, leading to the formation of structures described as the onion bulb [46]. Myelin sheath also detaches from the basal lamina of neurons to disintegrate into myelin debris [43] before the Schwann cells that are chronically denervated likely undergo apoptosis, leaving behind the basal lamina as a fingerprint of the process [47]. These features were evident in all ligated groups but were rare in sham control. Denervated Schwann cells produce cytokines or trophic factor and clear the debris by phagocytosis. Both Schwann cells and resident macrophages produce inflammatory mediators that recruit blood-borne macrophages to the injury site as the blood-nerve barrier permeability increases following axonal disintegration. These macrophages in turn phagocytose myelin and axon debris enabling axonal regeneration process to take place [48].

Expression of c-*fos* in four regions of the brain involved in the nociceptive pathway was demonstrated in mice that were not subjected to nociceptive assay to prevent the possibility of c-*fos* expression evoked by the external stimuli. This was standardised by providing similar housing facilities, feeding and handling procedures to avoid stress in the animals. The c-*fos* expression therefore, represents the general neuronal activation in the brain regions at resting. Parafascicular nuclei is the main intralaminar nucleus of the thalamus that receives spinothalamic afferents [49] which then projects to the anterior cingulate cortex, providing a cortical substrate for the affective-motivational aspects on pain processing [50]. Amygdala on the other hand, is the terminal site of disynaptic nociceptive spino(trigemio) potoamygdaloid pathway with relay in the parabrachial area which is involved in the affective-emotional, behavioural, and autonomic reaction to noxious events [51]. Hippocampus formation following pain response may modify the processing of incoming nociceptive information [52] whereby the activation of the hippocampal region is a useful marker during chronic pain [53].

c-*fos* expression in cingulate cortex, parafascicular nuclei and amygdala increased in all the mice subjected to CCI. This outcome is similar to reports by Narita et al. [54], Takeda et al. [55], Min et al. [56] and Leita-Almeida et al. [57]. Higher c-*fos* expressions indicate higher neuronal activity at these three regions. The expression of this immediate gene protein is the same in all the CCI-induced mice with different number of ligation(s), further supporting our behavioural outcomes indicating that nociception at these brain regions are similar between groups. However, unaltered levels of c-*fos* in the hippocampus, similar to that reported by Narita et al. [54], is possibly due to reduced neuronal activity. It is reported that the hippocampus region, which has high number of corticosteroid receptors, is most sensitive to stress-induced glucocorticoids release, making it particularly plastic and vulnerable [58, 59]. Furthermore, hippocampal synaptic plasticity in neuropathic pain condition was evident when hippocampal long-term potentiation was impaired following peripheral nerve injury [60]. Injury to the peripheral nervous system causes down regulation of the β-adrenergic activity in the hippocampus. Lowered β-adrenergic activity impairs synaptic transmission in the hippocampal CA1 region, therefore reducing neuronal activity [60].

We did not particularly screen for the changes in c-*fos* expression at lumbar spinal cord, which is a limitation faced in this study. However, based on previous literatures, c-*fos* expression increased at the L3–L6 dorsal horn of the spinal cord 15 days post-CCI with one, two and four ligations with chromic gut suture compared to control [61]. A 161% to 360% increase in c-*fos* immunoreactivity at day 3 and 10, respectively after CCI with four ligations, however, returned to levels similar to sham control 20 days after CCI [37]. Higher number of c-*fos* 14 days post-CCI was apparent at the laminae I–II compared to the deeper laminae III–IV and laminae V of the spinal cord as most of the endings of the primary afferents are present at these regions [62, 63]. This increased neuronal activation is evoked by various modalities of peripheral noxious stimulation.

Action potential is generated at the peripheral sensory neurons upon a sensory input, transmitted to spinal cord and up the ascending pain pathway before being perceived as pain in the brain [64]. On the basis that the pain thresholds and degree of sciatic nerve degeneration appears to be at similar levels in CCI models developed with one, two, three and four ligations and that extent of injury leads to similar level of neuronal activation in the brain, it is unlikely for any form of pain upregulation or pain modulation to have occurred in between. Report on the c-*fos* expression in the brain provides sufficient evidence on pain levels surrogated by all these models, as pain is ultimately perceived here. Therefore, we could postulate that there would not be any notable difference in the c-*fos* expression in the dorsal horn of L4–L6 spinal cord in all groups subjected to CCI. Another limitation to this study is that we were unable to link time matching data for c-*fos* and behaviour data due to the variations in terms of animal models, neuropathic pain models, number of ligations and the c-*fos* screening regions of previous studies.

Staining of c-*fos* to represent pain states of these animals was another limitation of this study. This marker characterises neuronal activation due to general continuous and/or subsequent peripheral stimuli and does not provide details on specific nociceptive signalling. Therefore, investigation on other markers such as aspartate, glutamate, non-N-methyl-D-aspartate (NMDA), 2-amino-3-hydroxy-5-methyl-4-isoxazole-proprionic acid (AMPA) and kainic acid receptor levels is warranted [65]. This is due to the active control and modulatory activity of the glutamatergic

system and its receptor subunits in transmitting nociceptive information at different levels in the synapse [66, 67].

Even though neuropathic pain is mainly processed by the nervous system, the hypersensitivity that arises is due to the activation of immune response. As a response to nerve damage, resident immune cells, macrophages and mast cells are activated, which triggers production of proinflammatory cytokines principally IL-1β, IL-6 and TNF-α. Elevated levels of these cytokines in DRG, dorsal horn of spinal cord, and blood serum post-CCI has been extensively reported [5, 19, 68–70]. Glial cells are activated at sensory ganglia and central structures but are generally activated in only a few regions of the brain [71] and not the whole brain [72]. Glial cells play a role in the progression and maintenance of pain as well as in immunomodulation through production of anti-inflammatory cytokines such as transforming growth factor- (TGF-)β and IL-10 [73]. The activation of glial cells following CCI has also been widely studied [74, 75]. However, subjectivity of previous literature in terms of different glial markers screened at different time points of the injury deter us to make comparisons from those studies. The lack of data on glial markers or immune response in this study was also a limitation, as we could not deduce the extent of immune response that occurred due to the injury induced with different number of ligations.

In conclusion, these results provide direct evidence that CCI models developed with one, two, three and four ligation(s) to the sciatic nerve produces equal magnitude of pain, similar morphological alterations within the nerve as well as expression of c-*fos* in the supraspinal regions investigated in this study. We therefore suggest that single ligation is sufficient to establish the CCI-induced animal model of neuropathic pain. In addition, the use of a single ligation may improve consistency, reduce animal-to-animal variation, decrease surgical time, and minimise the use of anaesthetics for the procedure eventually reducing stress on the animals.

Acknowledgements This research was supported by Universiti Putra Malaysia under the Ministry of Science, Technology & Innovation, Science Fund Scheme (Grant 5450778) and is greatly appreciated.

Compliance with Ethical Standards

Conflict of interest The authors have no conflicts of interests to declare.

Ethical Approval All procedures performed in this study involving animals were in accordance with the ethical standards of Institutional Animal Care and Use Committee (IACUC) of Universiti Putra Malaysia, at which the studies were conducted.

References

1. Austin PJ, Wu A, Moalem-Taylor G (2012) Chronic constriction of the sciatic nerve and pain hypersensitivity testing in rats. J Vis Exp JoVE 61:3393
2. Starowicz K, Przewlocka B (2012) Modulation of neuropathic-pain-related behaviour by the spinal endocannabinoid/endovanilloid system. Philos Trans R Soc B 367:3286–3299
3. Colleoni M, Sacerdote P (2010) Murine models of human neuropathic pain. Biochim Biophys Acta 1802:924–933
4. George A, Kleinschnitz C, Zelenka M, Brinkhoff J, Stoll G, Sommer C (2004) Wallerian degeneration after crush or chronic constriction injury of rodent sciatic nerve is associated with a depletion of endoneurial interleukin-10 protein. Exp Neurol 188:187–191
5. Hu P, Bembrick AL, Keay KA, McLachlan EM (2007) Immune cell involvement in dorsal root ganglia and spinal cord after chronic constriction or transection of the rat sciatic nerve. Brain Behav Immun 21:599–616
6. Whiteside GT, Adedoyin A, Leventhal L (2008) Predictive validity of animal pain models? A comparison of the pharmacokinetic-pharmacodynamic relationship for pain drugs in rats and humans. Neuropharmacology 54:767–775
7. Bennett GJ, Xie YK (1988) A peripheral mononeuropathy in rat that produces disorders of pain sensation like those seen in man. Pain 33:87–107
8. Ma W, Eisenach JC (2003) Chronic constriction injury of sciatic nerve induces the up-regulation of descending inhibitory noradrenergic innervation to the lumbar dorsal horn of mice. Brain Res 970:110–118
9. Kleinschnitz C, Hofstetter HH, Meuth SG, Braeuninger S, Sommer C, Stoll G (2006) T cell infiltration after chronic constriction injury of mouse sciatic nerve is associated with interleukin-17 expression. Exp Neurol 200:480–485
10. Lindenlaub T, Teuteberg P, Hartung T, Sommer C (2000) Effects of neutralizing antibodies to TNF-alpha on pain-related behavior and nerve regeneration in mice with chronic constriction injury. Brain Res 866:15–22
11. Ramer MS, Kawaja MD, Henderson JT, Roder JC, Bisby MA (1998) Glial overexpression of NGF enhances neuropathic pain and adrenergic sprouting into DRG following chronic sciatic constriction in mice. Neurosci Lett 251:53–56
12. Uçeyler N, Tscharke A, Sommer C (2007) Early cytokine expression in mouse sciatic nerve afterchronic constriction nerve injury depends on calpain. Brain Behav Immun 21:553–560
13. Zhang W, Xiao-Feng S, Jin-Hua B, Xiso-Jie L, Liu-Ping W, Zheng-Liang M, Xiao-Ping G (2013) Activation of mTOR in the spinal cord is required for pain hypersensitivity induced by chronic constriction injury in mice. Pharmacol Biochem Behav 111:64–70
14. Shimoyama M, Tanaka K, Hasua F, Shimoyama N (2002) A mouse model of neuropathic cancer pain. Pain 99:167–174
15. Ming-Tatt L, Khalivulla SI, Akhtar MN, Lajis N, Perimal EK, Akira A, Ali DI, Sulaiman MR (2013) Anti-hyperalgesic effect of a benzilidine-cyclohexanone analogue on a mouse model of chronic constriction injury-induced neuropathic pain: participation of the κ-opioid receptor and KATP. Pharmacol Biochem Behav 114–115:58–63
16. Zulazmi NA, Gopalsamy B, Farouk AAO, Sulaiman MR, Bharatham BH, Perimal EK (2015) Antiallodynic and antihyperalgesic effects of zerumbone on a mouse model of chronic constriction injury-induced neuropathic pain. Fitoterapia 105:215–221
17. Chia JSM, Omar Farouk AA, Mohamad AS, Sulaiman MR, Perimal EK (2016) Zerumbone alleviates chronic constriction

injury-induced allodynia and hyperalgesia through serotonin 5-HT receptors. Biomed Pharmacother 83:1303–1310
18. Campbell JN, Meyer RA (2006) Mechanisms of neuropathic pain. Neuron 52:77–92
19. Moalem G, Tracey DJ (2006) Immune and inflammatory mechanisms in neuropathic pain. Brain Res Rev 51:240–264
20. Hunt SP, Pini A, Eva G (1987) Induction of c-fos-like protein in spinal cord neurons following sensory stimulation. Nature 32:632–634
21. Greenberg ME, Ziff EB, Greene LA (1986) Stimulation of neuronal acetylcholine receptors induces rapid gene transcription. Science 234:80–83
22. Gao YJ, Ji RR (2009) c-Fos or pERK, which is a better marker for neuronal activation and central sensitization after noxious stimulation and tissue injury? Open Pain J 2:11–17
23. Vadakkan KI, Jia YH, Zhuo M (2005) A behavioral model of neuropathic pain induced by ligation of the common peroneal nerve in mice. J Pain 6:747–756
24. Nadal X, Baños JE, Kieffer BL, Maldonado R (2006) Neuropathic pain is enhanced in δ-opioid receptor knockout mice. Eur J Neurosci 23:830–834
25. Randall LO, Selitto JJ (1957) cA method for measurement of analgesic activity on inflamed tissue. Arch Int Pharm Ther 111:409–419
26. Hargreaves K, Dubner R, Brown F, Flores C, Joris J (1988) A new and sensitive method for measuring thermal nociception in cutaneous hyperalgesia. Pain 32:77–88
27. Liang C, Tao Y, Shen C, Tan Z, Xiong WC, Mei L (2012) Erbin is required for myelination in regenerated axonsafter injury. J Neurosci 32:15169–15180
28. Paxinos G, Franklin KBJ (1997) The mouse brain in stereotaxic coordinates. Academic Press, San Diego
29. van der Wal S, Cornelissen L, Behet M, Vanekar M, Steegers M, Vissers K (2015) Behavior of neuropathic pain in mice following chronic constriction injury comparing silk and catgut ligatures. SpringerPlus 4(1):225
30. Robinson I, Meert TF (2005) Stability of neuropathic pain symptoms in partial sciatic nerve ligation in rats is affected by suture material. Neurosci Lett 373:125–129
31. Vissers K, De Jongh R, Hoffmann V, Heylen R, Crul B, Meert T (2003) Internal and external factors affecting the development of neuropathic pain in rodents. Is it all about pain? Pain Pract 3:326–342
32. Clatworthy AL, Illich PA, Castro GA, Walters ET (1995) Role of peri-axonal inflammation in the development of thermal hyperalgesia and guarding behaviour in a rat model of neuropathic pain. Neurosci Lett 184:5–8
33. Olsson Y, Kristensson K (1973) The perineurium as a diffusion barrier to protein tracers following trauma to nerves. Acta Neuropathol 23:105–111
34. Zimmermann M (2001) Pathobiology of neuropathic pain. Eur J Pharmacol 429:23–37
35. Maves TJ, Pechman PS, Gebhart GF, Meller ST (1993) Possible chemical contribution from chromic gut sutures produces disorders of pain sensation like those seen in man. Pain 54:57–69
36. Grace PM, Hutchinson MR, Manavis J, Somogyi AA, Rolan PE (2010) A novel animal model of graded neuropathic pain: utility to investigate mechanisms of population heterogeneity. J Neurosci Methods 193:47–53
37. Kajander KC, Pollock CH, Berg H (1996) Evaluation of hindpaw position in rats during chronic constriction injury (CCI) produced with different suture materials. Somatosens Mot Res 13:95–101
38. Yamashita T, Sakuma Y, Kato Y, Kotani J (2004) Effect of different suture materials on the chronic constriction injury model. J Osaka Dent Univ 38:89–94
39. Postlethwait R (1970) Long-term comparative study of nonabsorbable sutures. Ann Surg 171:892
40. Jaggi AS, Singh N (2011) Exploring the potential of telmisartan in chronic constriction injury-induced neuropathic pain in rats. Eur J Pharmacol 667:215–221
41. Starowicz K, Mousa SA, Obara I, Chocyk A, Przewlocki R, Wedzony K, Machelska H, Przewlocka B (2009) Peripheral antinociceptive effects of MC4 receptor antagonists in rat model of neuropathic pain—a biochemical and behavioural study. Pharmacol Rep 61:1086–1095
42. Coleman MP, Freeman MR (2010) Wallerian degeneration. Wld(S), and Nmnat. Annu Rev Neurosci 1802:245–267
43. Gaudet AD, Popovich PG, Ramer MS (2011) Wallerian degeneration: gaining perspective on inflammatory events after peripheral nerve injury. J Neuroinflammation 8:110
44. Gupta R, Nassiri N, Hazel A, Bathen M, Tahseen M (2012) Chronic nerve compression alters Schwann cell myelin architecture in a murine model. Muscle Nerve 45:231–241
45. Beirowski B, Adalbert R, Wagner D, Grumme DS, Addicks K, Ribchester RR, Coleman MP (2005) The progressive nature of Wallerian degeneration in wild-type and slow Wallerian degeneration (WldS) nerves. BioMed Central Neurosci 6:6
46. Neely JG, Hough JV (1988) Histologic findings in two very small intracanalicular solitary schwannomas of the eight nerve: II. "Onion bulbs". Am J Otolaryngol 9:216–221
47. Low PA (1977) The evolution of "onion bulbs" in the hereditary hypertrophic neuropathy of the Trembler mouse. Neuropathol Appl Neurobiol 3:81–92
48. Griffin JW, Thompson WJ (2008) Biology and pathology of nonmyelinating Schwann cells. Glia 56:1518–1531
49. Cross SA (1994) Pathophysiology of Pain. Mayo Clin Proc 69:375–383
50. Vogt BA, Sikes RW, Vogt LJ (1993) Anterior cingulate cortex and the medial pain system. In: Vogt BA, Gabriel M (eds) Neurobiology of cingulate cortex and limbic thalalmus. Birkhauser, Boston, pp 313–344
51. Bernard JF, Besson JM (1990) The spino(trigemio)pontoamygdaloid pathway: electrophysiological evidence for an involvement in pain processes. J Neurophysiol 63:473–490
52. Soleimannejad E, Semnanian S, Fathollahi Y, Naghdi N (2006) Microinjection of ritanserin into the dorsal hippocampal CA1 and gyrus decrease nociceptive behavior in adult male rat. Behav Brain Res 168:221–225
53. Duric V, McCarson KE (2005) Hippocampal neurokinin-1 receptor and brain-derived neurotrophic factor gene expression is decreased in rat models of pain and stress. Neurosci Lett 133:999–1006
54. Narita M, Ozaki S, Narita M, Ise Y, Yajima Y, Suzuki T (2003) Change in the expression of c-fos in the rat brain following sciatic nerve ligation. Neurosci Lett 352:231–233
55. Takeda R, Watanabe Y, Ikeda T, Abe H, Ebihara K, Matsuo H, Nonaka H, Hashiguchi H, Nishimori T, Ishida Y (2009) Analgesic effect of milnacipran is associated with c-Fos expression in the anterior cingulate cortex in the rat neuropathic pain model. Neurosci Res 64:380–384
56. Min JH, Park CM, Moon DE, Kim SN, Chung CW, Kim KH (2001) Fos expression in the brain of neuropathic pain rats. Korean J Anesthesiol 41:229–238
57. Leita-Almeida H, Guimarães MR, Cerqueira JJ, Ribeiro-Costa N, Martins HA, Sousa N, Almeida A (2014) Asymmetric c-fos expression in the ventral orbital cortex is associated with impaired reversal learning in a right-sided neuropathy. Mol Pain 10:41
58. Sapolsky RM (2003) Stress and Plasticity in the Limbic System. Neurochem Res 28:1735–1742
59. Krugers HJ, Lucassen PJ, Henk Karst H, Joëls M (2010) Chronic stress effects on hippocampal structure and synaptic function:

relevance for depression and normalization by anti-glucocorticoid treatment. Front Synaptic Neurosci 2:1–10
60. Kodama D, Ono H, Tanabe M (2007) Altered hippocampal long-term potentiation after peripheral nerve injury in mice. J Pharmacol 574:127–132
61. Tao T, Wei MY, Guo XW, Zhang J, Yang LY, Zheng H (2019) Modulating cAMP responsive element binding protein 1 attenuates functional and behavioural deficits in rat model of neuropathic pain. Eur Rev Med Pharmacol Sci 23:2602–2611
62. Yu-Chuan T, Edmund S, Hsing-Hong C, Li-Kai W, Chi-Hsien C (2002) Effect of intrathecal octreotide on thermal hyperalgesia and evoked spinal c-Fos expression in rats with sciatic constriction injury. Pain 99:407–413
63. Maeda Y, Ikeuchia M, Wacnik Kathleen A, Sluka KA (2009) Increased c-fos immunoreactivity in the spinal cord and brain following spinal cord stimulation is frequency-dependent. Brain Res 1259:40–50
64. Cross SA (1994) Pathophysiology of pain. Mayo Clin Proc 69:375–383
65. Gong K, Kung LH, Magni G, Bhargava A, Jasmin L (2014) Increased response to glutamate in small diameter dorsal root ganglion neurons after sciatic nerve injury. PLoS ONE 9(4):e95491. https://doi.org/10.1371/journal.pone.0095491
66. Bardoni R (2013) Role of presynaptic glutamate receptors in pain transmission at the spinal cord level. Curr Neuropharmacol 11(5):477–483
67. Osikowicz M, Mika J, Przewlocka B (2013) The glutamatergic system as a target for neuropathic pain relief. Exp Physiol 98(2):372–384
68. Lee HL, Lee KM, Son SJ, Hwang SH, Cho HJ (2004) Temporal expression of cytokines and their receptors mRNAs in a neuropathic pain model. NeuroReport 15:2807–2811
69. Gopalsamy B, Farouk AAO, Sulaiman MR, Mohamad TAST, Perimal EK (2017) Antiallodynic and antihyperalgesic activities of zerumbone via the suppression of IL-1β, IL-6, and TNF-α in a mouse model of neuropathic pain. J Pain Res 10:2605–2619
70. Dubovy P, Jancalek R, Klusakova I, Svizenska I, Pejchalova K (2006) Intra- and extraneuronal changes of immunofluorescence staining for TNF-alpha and TNFR1 in the dorsal root ganglia of rat peripheral neuropathic pain models. Cell Mol Neurobiol 26:1205–1217
71. Taylor AM, Mehrabani S, Liu S, Taylor AJ, Cahill CM (2017) Topography of microglial activation in sensory-and affect-related brain regions in chronic pain. J Neurosci Res 95:1330–1335
72. Barcelon EE, Cho W, Jun SB, Lee SJ (2019) Brain microglial activation in chronic pain-associated affective disorder. Front Neurosci 13:213
73. Ledeboer A, Brevé JJ, Poole S, Tilders FJ, Vandam AM (2000) Interleukin-10, interleukin-4, and transforming growth factor-beta differentially regulate lipopolysaccharide-induced production of pro-inflammatory cytokines and nitric oxide in co-cultures of rat astroglial and microglial cells. Glia 30(2):134–142
74. Giardini AC, dos Santos FM, da Silva JT, de Oliveira ME, Martins DO, Chacur M (2017) Neural mobilization treatment decreases glial cells and brain-derived neurotrophic factor expression in the central nervous system in rats with neuropathic pain induced by CCI in rats. Pain Res Manag. https://doi.org/10.1155/2017/7429761
75. Bian J, Zhang Y, Liu Y, Li Q, Tang H-B, Liu Q (2019) P2Y6 receptor-mediated spinal microglial activation in neuropathic pain. Pain Res Manag. https://doi.org/10.1155/2019/2612534